

Parallel ancient genomic transects reveal complex population history of early European farmers

Mark Lipson,^{1,†,*} Anna Szécsényi-Nagy,^{2,†,*} Swapan Mallick,^{1,3} Annamária Pósa,² Balázs Stégmár,² Victoria Keerl,⁴ Nadin Rohland,¹ Kristin Stewardson,^{1,5} Matthew Ferry,^{1,5} Megan Michel,^{1,5} Jonas Oppenheimer,^{1,5} Nasreen Broomandkhoshbacht,^{1,5} Eadaoin Harney,^{1,5} Susanne Nordenfelt,¹ Bastien Llamas,⁶ Balázs Gusztáv Mende,² Kitty Köhler,² Krisztián Oross,² Mária Bondár,² Tibor Marton,² Anett Oszrás,² János Jakucs,² Tibor Paluch,⁷ Ferenc Horváth,⁷ Piroška Csengeri,⁸ Judit Koós,⁸ Katalin Sebők,⁹ Alexandra Anders,⁹ Pál Raczky,⁹ Judit Regenye,¹⁰ Judit P. Barna,¹¹ Szilvia Fábián,¹² Gábor Serlegi,² Zoltán Toldi,¹³ Emese Gyöngyvér Nagy,¹⁴ János Dani,¹⁴ Erika Molnár,¹⁵ György Pálfi,¹⁵ László Márk,^{16,17,18,19} Béla Melegh,^{18,20} Zsolt Bánfai,^{18,20} Javier Fernández-Eraso,²¹ José Antonio Mujika-Alustiza,²¹ Carmen Alonso Fernández,²² Javier Jiménez Echevarría,²² Ruth Bollongino,⁴ Jörg Orschiedt,^{23,24} Kerstin Schierhold,²⁵ Harald Meller,²⁶ Alan Cooper,^{6,27} Joachim Burger,⁴ Eszter Bánffy,^{2,28} Kurt W. Alt,²⁹ Carles Lalueza-Fox,³⁰ Wolfgang Haak,^{6,31} David Reich^{1,3,5,*}

¹Department of Genetics, Harvard Medical School, Boston, MA 02115, USA

²Institute of Archaeology, Research Centre for the Humanities, Hungarian Academy of Sciences, Budapest H-1097, Hungary

³Medical and Population Genetics Program, Broad Institute of MIT and Harvard, Cambridge, MA 02142,

USA

⁴Institute of Organisms and Molecular Evolution, Johannes Gutenberg University Mainz, Mainz D-55128, Germany

⁵Howard Hughes Medical Institute, Harvard Medical School, Boston, MA 02115, USA

⁶Australian Centre for Ancient DNA, School of Biological Sciences, University of Adelaide, Adelaide, SA 5005, Australia

⁷Móra Ferenc Museum, H-6720 Szeged, Hungary

⁸Herman Ottó Museum, H-3529 Miskolc, Hungary

⁹Institute of Archaeological Sciences, Eötvös Loránd University, Budapest H-1088, Hungary

¹⁰Laczkó Dezső Museum, H-8200 Veszprém, Hungary

¹¹Balaton Museum, H-8360 Keszthely, Hungary

¹²Department of Archaeological Excavations and Artefact Processing, Hungarian National Museum, Budapest H-1088, Hungary

¹³Jósa András Museum, H-4400 Nyíregyháza, Hungary

¹⁴Déri Museum, H-4026 Debrecen, Hungary

¹⁵Department of Biological Anthropology, Szeged University, H-6726 Szeged, Hungary

¹⁶Department of Biochemistry and Medical Chemistry, University of Pécs, Pécs H-7624, Hungary

¹⁷Imaging Center for Life and Material Sciences, University of Pécs, Pécs H-7624, Hungary

¹⁸Szentágothai Research Center, University of Pécs, Pécs H-7624, Hungary

¹⁹PTE-MTA Human Reproduction Research Group, Pécs H-7624, Hungary

²⁰Department of Medical Genetics and Szentágothai Research Center, University of Pécs, Pécs H-7624, Hungary

²¹Department of Geography, Prehistory, and Archaeology, University of the Basque Country, Investigation Group IT622-13, 01006 Vitoria-Gasteiz, Spain

²²CRONOS SC, 09007 Burgos, Spain

²³Department of Prehistoric Archaeology, Free University of Berlin, 14195 Berlin, Germany

²⁴Curt-Engelhorn-Centre Archaeometry gGmbH, 68159 Mannheim, Germany

²⁵Commission for Westphalian Antiquities, Westphalia-Lippe Regional Association, 48157 Münster, Germany

²⁶State Office for Heritage Management and Archaeology Saxony-Anhalt and State Heritage Museum,

D-06114 Halle, Germany.

²⁷Environment Institute, University of Adelaide, Adelaide, SA 5005, Australia

²⁸Romano-Germanic Commission, German Archaeological Institute, D-60325 Frankfurt am Main, Germany

²⁹Center of Natural and Cultural History of Man, Danube Private University, A-3500 Krems-Stein, Austria

³⁰Institute of Evolutionary Biology (CSIC-UPF), 08003 Barcelona, Spain

³¹Department of Archaeogenetics, Max Planck Institute for the Science of Human History, 07745 Jena, Germany

[†]These authors contributed equally to this work

*Email: mlipson@genetics.med.harvard.edu, szecsenyi-nagy.anna@btk.mta.hu, reich@genetics.med.harvard.edu

Ancient DNA studies have established that European Neolithic populations were descended from Anatolian migrants who received a limited amount of admixture from resident hunter-gatherers. Many open questions remain, however, about the spatial and temporal dynamics of population interactions and admixture during the Neolithic period. Using the highest-resolution genome-wide ancient DNA data set assembled to date—a total of 177 samples, 127 newly reported here, from the Neolithic and Chalcolithic of Hungary (6000–2900 BCE, $n = 98$), Germany (5500–3000 BCE, $n = 42$), and Spain (5500–2200 BCE, $n = 37$)—we investigate the population dynamics of Neolithization across Europe. We find that genetic diversity was shaped predominantly by local processes, with varied sources and proportions of hunter-gatherer ancestry among the three regions and through time. Admixture between groups with different ancestry profiles was pervasive and resulted in observable population transformation across almost all cultural transitions. Our results shed new light on the ways that gene flow reshaped European populations through-

out the Neolithic period and demonstrate the potential of time-series-based sampling and modeling approaches to elucidate multiple dimensions of historical population interactions.

The population dynamics of the Neolithization process are of great importance for understanding European prehistory [1–5]. The first quantitative model of the Neolithic transition to integrate archaeological and genetic data was the demic diffusion hypothesis [1], which posited that growing population densities among Near Eastern farmers led to a range expansion that spread agriculture to Europe. Ancient DNA analysis has validated major migrations from populations related to Neolithic Anatolians as driving the arrival of farming in Europe [6–13], but the demic diffusion model does not account for the complexities of the interactions between farmers and hunter-gatherers in Europe throughout the Neolithic [2, 3, 14–16]. For example, ancient DNA has shown that farmers traversed large portions of Europe with limited initial admixture from hunter-gatherers [8, 10, 12, 13, 17], and furthermore that farmers and hunter-gatherers lived in close proximity in some locations long after the arrival of agriculture [18, 19]. However, genetic data have yet to be used systematically to model the population interactions and transformations during the course of the Neolithic period. Key open questions include whether migrating farmers mixed with hunter-gatherers at each stage of the expansion, and if so how soon after arriving. Additionally, while it has previously been shown that hunter-gatherer ancestry among farmers in several parts of Europe had increased by the Middle Neolithic [10, 12, 13, 20], it is currently unclear whether this was a continuous or discrete process and furthermore whether it involved a continent-wide phenomenon or a variety of parallel, local events.

We compiled a high-resolution data set of 177 Neolithic and Chalcolithic European genomes (pre-dating the arrival of steppe ancestry in the third millennium BCE [10]) from what are now Hungary, Germany, and Spain, of which 127 individuals are newly

reported here, 38 with new direct radiocarbon dates (Figure 1A, B; Extended Data Table 1; Supplementary Tables 1, 2; Supplementary Information sections 1–3). We enriched for DNA fragments covering a set of ~ 1.23 million single nucleotide polymorphism (SNP) targets [12, 21] (Methods) and obtained largely high-quality data, with at least 100,000 SNPs hit at least once (average coverage ~ 0.1 or higher) for 88 of the 127 samples. The majority (88) of our new samples comprise an approximately 3000-year transect of the prehistory of the Carpathian Basin (Supplementary Information section 1), from both the eastern (Great Hungarian Plain, or Alföld) and western (Transdanubia) portions of present-day Hungary: 7 Early Neolithic (EN, ~ 6000 – 5500 BCE) Starčevo (western) and Körös (eastern) individuals; 33 Middle Neolithic (MN, ~ 5500 – 5000 BCE) individuals from the Transdanubian (LBKT) and Alföld (ALPc) Linearbandkeramik cultures and from the Vinča culture in southern Transdanubia; 20 Late Neolithic (LN, ~ 5000 – 4500 BCE) individuals (eastern Tisza, western Sopot and Lengyel, the latter two grouped together as Transdanubian LN, or TDLN); and 28 Tiszapolgár, Balaton-Lásinja, Hunyadhalom, Protoboleráz, and Baden individuals from the Chalcolithic period (CA, ~ 4500 – 2850 BCE). From what is now Germany, we generated data for 15 new Linearbandkeramik (LBK) EN (~ 5500 – 4850 BCE) and eight new MN (~ 4600 – 3000 BCE) individuals (with new libraries for an additional nine LBK for which we have previously reported data), while from Spain, we sequenced two new EN (~ 5500 – 4500 BCE) and 14 new CA (~ 3000 – 2200 BCE) individuals. After quality control (Methods), we retained 110 samples, which we merged with 50 Neolithic individuals from the literature [9, 10, 12, 22, 23]. For population genetic analyses, we focused on a subset of 151 individuals from 15 population groupings for which we had the highest-quality data. We co-analyzed these samples with 25 Neolithic individuals (~ 6500 – 6000 BCE) from northwestern Anatolia [12] to represent the ancestors of the first European farmers (FEF; Supplementary Information section 4)

and four primary European hunter-gatherer individuals (“western hunter-gatherers,” or WHG): the ~5700 BCE “KO1” from Hungary [12, 22], the ~5900 BCE “La Braña 1” (LB1) from Spain [12, 24], the ~6100 BCE “Loschbour” from Luxembourg [9], and the ~12,000 BCE “Villabruna” from northeastern Italy [25].

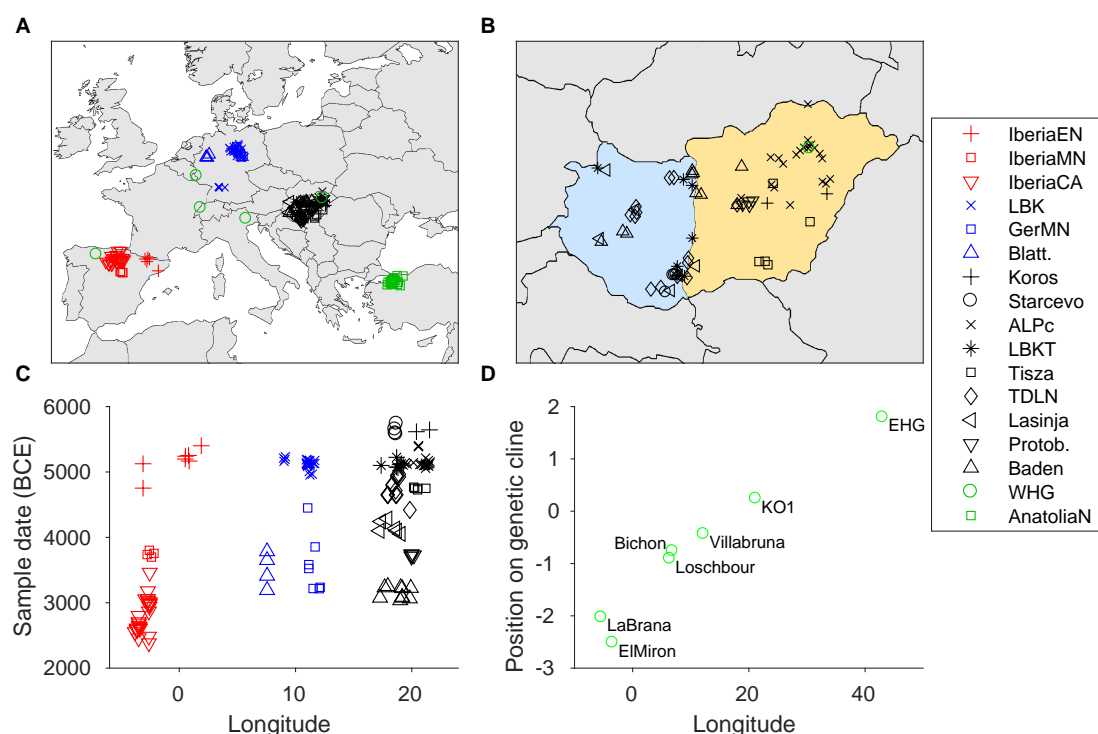


Figure 1. Spatial and temporal contexts of European Neolithic samples. (A), (B) Locations of samples used for analyses, with closeup of Hungary (orange shading for Alföld and light blue for Transdanubia). (C) Sample dates arranged by longitude. (D) Hunter-gatherer genetic cline (derived from MDS analysis; Supplementary Information section 5) as a function of longitude. Random jitter is added to separate overlapping positions in (A)–(C). GerMN, Germany MN; Blatt., Blätterhöhle; Protob., Protoboleráz.

A principal component analysis (PCA [26]) of our samples showed that, as expected, all of the Neolithic individuals fall along a cline of admixture between FEF and WHG,

with varying proportions of hunter-gatherer ancestry (Extended Data Figure 1). All studied population groups are consistent with a common origin in Anatolia (Supplementary Information section 4), and differentiation among the ancestral farmer populations in the three regions is low (Extended Data Figure 1). To investigate genetic structure within the source population(s) of hunter-gatherer ancestry, we combined the four primary WHG individuals with other hunter-gatherers (eastern hunter-gatherers, or “EHG,” ~7000–5000 BCE from Russia [10,12]; “Bichon,” ~10,000 BCE from Switzerland [27]; and “El Mirón,” ~17,000 BCE from Spain [25]) along an approximate east–west transect across Europe. We computed pairwise outgroup f_3 -statistics, performed multidimensional scaling (MDS) on the resulting matrix, and converted the MDS positions to polar coordinates (Supplementary Information section 5). The correlation between genetic structure and longitude revealed by this analysis (Figure 1D) suggests that our reference samples can reasonably be used to define a geographic cline among hunter-gatherers within Europe. Computing f_4 -statistics measuring shared drift between our Neolithic samples and the WHG individuals, we observed an increasing trend in hunter-gatherer ancestry over time in each region [10–12], although at a slower rate in Hungary than in Germany and Spain, and with limited intra-population structure or heterogeneity (Figure 2A; Supplementary Information section 6). We find that this hunter-gatherer ancestry is more similar to the eastern WHG individuals (KO1 and Villabruna) farther east and more similar to the western WHG individuals (LB1 and Loschbour) farther west (Figure 2B). While this pattern does not demonstrate directly where mixture between hunter-gatherers and farmers took place, it suggests that hunter-gatherer ancestry in farmers was to a substantial extent derived from populations from relatively close to where they lived.

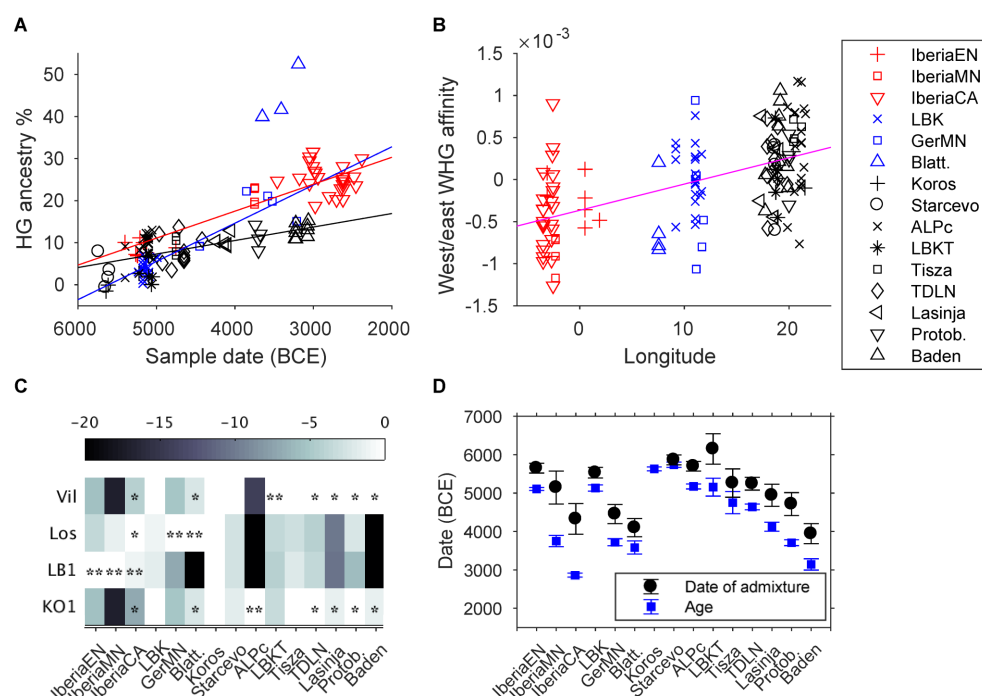


Figure 2. Admixture parameters for test individuals and populations. (A) Estimated individual hunter-gatherer ancestry versus sample date, with best-fitting regression lines for each region (excluding Blätterhöhle). Standard errors are around 2% for hunter-gatherer ancestry and 100 years for dates (Methods; Extended Data Table 1). Individual Bla8 (~74% hunter-gatherer ancestry) is omitted for scale. (B) Relative affinity of hunter-gatherer ancestry in Neolithic individuals, measured as $f_4(\text{LB1} + \text{Loschbour}, \text{KO1} + \text{Villabruna}; \text{Anatolia}, X)$ (positive, more similar to eastern WHG; negative, more similar to western WHG; standard errors $\sim 5 \times 10^{-4}$), with best-fitting regression line (nominal $p \sim 10^{-11}$, unadjusted for non-independence among samples). Within-region correlations are not significant (Hungary $p \sim 0.1$), whereas the three regions in aggregate differ from each other at $|Z| > 3$. (C) Relative log-likelihood of admixture graph models fitting each population as a mixture of FEF and one of the four WHG individuals (Los, Loschbour; Vil, Villabruna). Asterisks denote statistical significance ($p < 0.05$; Supplementary Information section 6), with single asterisks for significant components whose source is not uniquely identified (Extended Data Table 2). (D) Population-level average sample ages and dates of admixture, plus or minus two standard errors. Due to heterogeneity, we omit the outlier individuals Bla28 (Blätterhöhle) and GEN61 (Protoboleráz) in the dates.

To analyze admixed hunter-gatherer ancestry more formally, we modeled Neolithic farmers in an admixture graph framework. We started with a “scaffold” model (Extended Data Figure 3) consisting of Neolithic Anatolians, the four reference WHG individuals, and two outgroups (Mbuti and Kostenki 14 [25, 28]). We observed discrete signals of admixture in LB1 and KO1 via f_3 - and f_4 -statistics [29], and both fit best as admixed in the scaffold model, LB1 with ancestry from a deeper European hunter-gatherer lineage and KO1 with a small proportion of FEF admixture (Supplementary Information section 6). We then added each Neolithic population to this model in turn, fitting them as a mixture of FEF and either one or two hunter-gatherer ancestry components. To check for robustness, we repeated our analyses using transversions or outgroup-ascertained SNPs only, with in-solution capture data for Loschbour, and with additional or alternative hunter-gatherers in the model (Extended Data Table 2; Supplementary Information section 6), and in all cases the results were qualitatively consistent. We find that almost all ancient groups from Hungary have ancestry significantly closest to one of the more eastern WHG individuals (either KO1 or Villabruna); the samples from present-day Germany have greatest affinity to Loschbour; and all three Iberian groups contain LB1-related ancestry (Figure 2C; Extended Data Table 2). This pattern implies that admixture into European farmers occurred multiple times from local hunter-gatherer populations. Moreover, combining the proportions and sources of hunter-gatherer ancestry, populations from the three regions are distinguishable at all stages of the Neolithic. Thus, any further migrations that may have occurred after the initial spread of farming were not substantial enough within the studied regions to disrupt the observed heterogeneity.

Additional insights about population interactions can be gained by studying the dates of admixture events. We used *ALDER* [30] to estimate dates of admixture for Neolithic individuals based on the recombination-induced breakdown of contiguous blocks of FEF

and WHG ancestry over time (Extended Data Table 1). The *ALDER* algorithm is not able to accommodate large amounts of missing data, so we developed a strategy for running it with the relatively low coverage of ancient DNA (Supplementary Information section 7). To obtain calendar dates of admixture (Figure 2D), we combine the *ALDER* results (in generations in the past) with the ages of the Neolithic individuals, assuming an average generation time of 28 years [31,32]. These dates are based on a model of a single wave of admixture, which means that if the true history for a population includes multiples waves or continuous admixture, we will obtain an intermediate value. Additionally, while the primary signal is due to admixture between farmers and hunter-gatherers, mixture among farmers can also be detected if the groups have different proportions of hunter-gatherer ancestry, meaning that inferred dates, especially for later populations, may not all reflect admixture between farmers and unadmixed hunter-gatherers.

For our most complete time series, from Hungary, we infer admixture dates throughout the Neolithic that are on average mostly 18–30 generations old (500–840 years), indicating a degree of ongoing population transformation and admixture ((Figure 2D; Extended Data Table 3). This pattern is accompanied by a gradual increase in hunter-gatherer ancestry over time, although never reaching the levels observed in MN Germany or Iberia (Figure 2A). While five of the six EN individuals from Hungary do not have significantly more hunter-gatherer ancestry than Neolithic Anatolians (Figure 2A; Extended Data Table 1), one Starčevo sample, BAM17b, is inferred to have $7.9 \pm 1.7\%$ hunter-gatherer ancestry and a very recent *ALDER* date of 4.5 ± 1.9 generations (5865 ± 65 BCE; 2.9 ± 1.6 generations using a group-level estimate; Extended Data Table 3), consistent with his having had one or two hunter-gatherer ancestors in the last several generations. We also infer an average admixture date of 5700 ± 65 BCE for the ALPc MN, again suggesting that in Hungary, interaction between Anatolian migrants and local HGs began in the

Early Neolithic (cf. [14, 33–35]). The greatest differences between Alföld and Transdanubia are observed in the MN, with substantially more hunter-gatherer ancestry in ALPc than LBKT (Figure 2; Extended Data Table 2), and overall, we observe slight trends toward more hunter-gatherer ancestry to the north and east (Extended Data Figure 2), as expected based on the greater archaeological evidence of hunter-gatherer settlement and interactions [33]. By the LN and CA, however, and especially in the Baden period (when the region became culturally unified [36]) our results are broadly similar over the two halves of present-day Hungary.

From Germany, we analyzed a large sample of the EN LBK culture and 11 individuals from the MN period, four of them from the Blätterhöhle site [18]. The average date of admixture for LBK (5530 ± 70 BCE) is more recent than the dates for EN/MN populations from Hungary, and the total hunter-gatherer ancestry proportion in LBK ($\sim 4\text{--}5\%$) is intermediate between LBKT and ALPc. This ancestry is most closely related to a combination of KO1 and Loschbour, although the assignment of the hunter-gatherer source(s) is not statistically significant (Figure 2B; Extended Data Table 2). These results are consistent with genetic and archaeological evidence for LBK origins from the early LBKT [35], followed by additional, Central European WHG admixture after about 5500 BCE. Our “Germany MN” grouping shows increased hunter-gatherer ancestry ($\sim 17\%$, most closely related to Loschbour) and a more recent average date of admixture, reflecting gene flow from hunter-gatherers after the LBK period. We successfully sequenced a total of 16 Blätterhöhle MN samples, many of them with distinct individual labels from ref. [18], although surprisingly, the genome-wide data indicated that these corresponded to only four unique individuals, for which we merged libraries to increase coverage: Bla28; Bla5 (same as Bla7, Bal13, Bla26(o), Bla30, and Bla54); Bla16 (same as Bla27 and Bla59); and Bla8 (same as Bla9, Bla11, Bla24, Bla26(x), and Bla45). Based on stable isotopes, the

first three of these were classified as farmers, while Bla8 had signatures associated with a hunter-gatherer-fisher lifestyle [18]. In accordance with previous results [18], we find that the group of MN farmers experienced admixture with hunter-gatherers, which we now estimate to have been at least 40%. We additionally observe admixture in the individual Bla8, with $\sim 25\%$ ancestry derived from farmers. Our results thus provide evidence of asymmetric gene flow between farmers and hunter-gatherers at Blätterhöhle centered around the relatively late date of 4100 ± 120 BCE (*ALDER* dates of 10–25 generations).

In Iberia, we again see widespread evidence of local hunter-gatherer admixture, with confidently inferred LB1-related ancestry in all three population groups (EN, MN, and CA). For Iberia EN, we infer an average admixture date of 5650 ± 65 BCE, which rises to 5860 ± 110 BCE when considering only the five oldest samples (of which the earliest, CB13 [23], has an individual estimate of 5890 ± 105 BCE). Given that farming is thought to have arrived in Spain around 5500 BCE [37], these dates suggest the presence of at least a small proportion of hunter-gatherer ancestry in earlier Cardial Neolithic populations acquired along their migration route (although our admixture graph analysis only confidently detected an LB1-related component). The later Iberians have large proportions of hunter-gatherer ancestry, approximately 23% for MN (from the site of La Mina, in north-central Iberia) and 27% for CA, and also relatively old *ALDER* dates (approximately 50 generations, or 1400 years), indicating that most of the admixture occurred well before their respective sample dates. Both populations have evidence of ancestry related to LB1 and to a different WHG individual, suggesting that in contrast to the earlier admixture, the large increase in hunter-gatherer ancestry between the EN and MN had a non-local origin.

Synthesizing our time series data, we compared the observed *ALDER* dates and hunter-gatherer ancestry proportions of Neolithic populations to those estimated for sim-

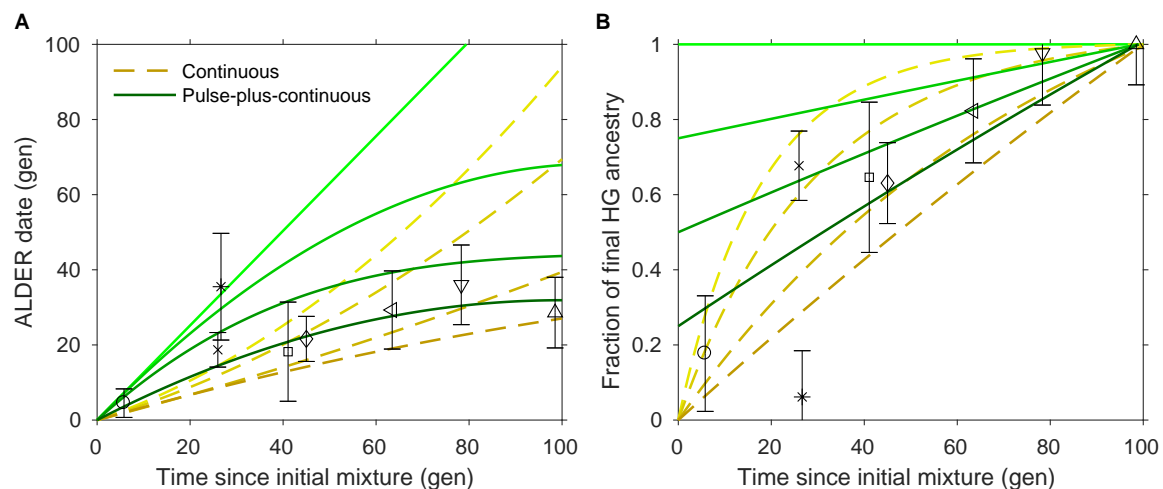


Figure 3. Admixture dates (A) and proportions (B) as a function of time for the Hungary time series and simulated data. Symbols are as in Figures 1 and 2, here showing population-level averages plus or minus two standard errors. Proportions and standard errors in (B) are normalized by the total hunter-gatherer ancestry in the most recent (rightmost) population in each region. Yellow dashed lines represent continuous admixture simulations: from top to bottom, diminishing 5% per generation, diminishing 3%, diminishing 1%, and uniform. Green solid lines represent pulse-plus-continuous admixture simulations: from top to bottom, all hunter-gatherer ancestry in a pulse at time zero; 3/4 of final hunter-gatherer ancestry in an initial pulse, followed by uniform continuous gene flow; 1/2 in initial pulse and the rest continuous; and 1/4 in initial pulse. Data for Germany and Iberia are shown in Extended Data Figure 4; see Supplementary Information section 8 for full details.

ulated data under different temporal admixture scenarios (Figure 3; Extended Data Figure 4; Supplementary Information section 8). We assumed dates of 5900 BCE (Hungary) and 5500 BCE (Germany and Spain) for the onset of mixture. While none of the scenarios match the data perfectly, a reasonably good fit for Hungary is provided by a model of an initial admixture pulse (approximately 1/4 of the total hunter-gatherer ancestry observed by the end of the time series) followed by continuous gene flow (bottom solid green curve in both panels of Figure 3). Alföld and Transdanubia should be considered as separate series, but their parameters follow mostly similar trajectories, with the exception of the MN, where LBKT has a relatively old admixture date (albeit with large uncertainty) and ALPc a relatively high hunter-gatherer ancestry proportion (possibly influenced by the bias of sampling in favor of the middle and northern parts of the Alföld). Overall, even after normalizing for the different total hunter-gatherer ancestry proportions in each region, we observe a high degree of local distinctiveness, for example in the older *ALDER* dates for Iberia MN/CA and the markedly higher hunter-gatherer ancestry in Blätterhöhle. Where the simulated scenarios do not align with the real data, we can use the results to constrain the possible admixture histories in each region, e.g., by rejecting the models of a single admixture pulse or uniform continuous admixture. We also note that while the simulated data are generated under a model of gene flow from an unadmixed hunter-gatherer source population into a series of farmer populations in a single line of descent, observed admixture could also reflect immigration of new farmer populations (either via their own previous hunter-gatherer admixture or new admixture between farming populations with different proportions of hunter-gatherer ancestry). Based on archaeological evidence, such a scenario is possible, for example, for the introduction of hunter-gatherer ancestry into TDLN from Southeastern European farmers via the dispersal of the northern Balkan Vinča or Sopot cultures to Transdanubia [14, 38, 39].

Our results provide greatly increased detail in understanding population interactions and admixture during the European Neolithic. In each of our three study regions, the arrival of farmers prompted admixture with local hunter-gatherers which unfolded over thousands of years: almost all sampled populations from subsequent time periods have more hunter-gatherer ancestry and more recent dates of admixture than their local predecessors, suggesting recurrent changes in genetic composition and significant hunter-gatherer gene flow beyond initial contact. These transformations left distinct signatures in each region, implying that they likely resulted from a complex web of local interactions rather than a uniform demographic phenomenon. Our transect of Hungary, in particular, with representative samples from many archaeological cultures across the region and throughout the Neolithic and Chalcolithic, illustrates the power of dense ancient DNA time series. Future work with similar data sets and statistical models promises to teach us much more about population transformations in space and time.

Methods

Experimental procedures

Prehistoric teeth and petrous bone samples from Hungary were taken under sterile conditions in the Hungarian Museums and anthropological collections. Sixty-six samples were documented, cleaned, and ground into powder in the Anthropological Department of the Johannes Gutenberg University of Mainz, during the course of the German Research Foundation project AL 287-10-1, and the other 20 were prepared in Budapest, in the Laboratory of Archaeogenetics of the Institute of Archaeology, Research Centre for the Humanities, Hungarian Academy of Sciences, following published protocols [35]. DNA was extracted in Budapest using 0.08–0.11g powder via published methods [40], using

High Pure Viral NA Large Volume Kit columns (Roche) [21, 41]. DNA extractions were tested by PCR, amplifying the 16117–16233 bp fragment of the mitochondrial genome, and visualized on a 2% agarose gel. DNA libraries were prepared from clean and successful extraction batches using UDG-half and no-UDG treated methods [10, 42]. We included milling (hydroxylapatite blanks to control for cleanness) and extraction negative controls in every batch. Barcode adapter ligated libraries were amplified with TwistAmp Basic (Twist DX Ltd), purified with Agencourt AMPure XP (Beckman Coulter), and checked on 3% agarose gel [10]. Library concentration was measured on a Qubit 2.0 fluorometer. Promising libraries after initial quality control analysis were shipped to Harvard Medical School, where further processing took place. All other samples were prepared similarly in dedicated clean rooms at Harvard Medical School and the University of Adelaide in accordance with published methods [10, 12, 21].

We initially screened the libraries by examining mitochondrial DNA (mtDNA) content via in-solution hybridization to a set of mtDNA probes [43], using a protocol described previously [10, 21]. Libraries with good screening results—limited evidence of contamination, reasonable damage profiles, and substantial coverage on targeted segments—were enriched for a genome-wide set of ~ 1.2 million SNPs [12, 21] and sequenced to greater depth. Raw sequencing data were processed by trimming bar codes and adapters, merging read pairs with at least 15 base pairs of overlapping sequence, and mapping to the human reference genome (version hg19). Reads were filtered for mapping and base quality, duplicate molecules were removed, and two terminal bases were clipped to eliminate damage (five for UDG-minus libraries) [10]. All libraries had a rate of at least 4.8% C-to-T substitutions in the final base of screening sequencing reads (Supplementary Table 1), consistent with damage patterns expected for authentic ancient DNA [42, 44]. Pseudo-haploid genotypes at each SNP were called by choosing one allele at random from among

mapped reads.

Mitochondrial DNA sequences were reassembled in Geneious R10 to rCRS [45] and RSRS [46], and SNPs with at least 3x coverage and a minimum variant frequency of 0.7 were called. The assembly and the resulting list of SNPs were double-checked against phylotree.org (mtDNA tree Build 17; 18 Feb 2016). Haplotype calls are given in Table SXX (in progress). On the Y chromosome, 15,100 SNPs were targeted and sequenced, and the detected derived and ancestral alleles were compared to the ISOGG Y-tree (www.isogg.org) version 12.34, updated on 5th February 2017. Haplogroup definitions are detailed in Supplementary Information section 3.

We merged libraries from the same individual (for those with more than one) and then combined our new samples with genome-wide data from the literature (ancient individuals as described and as listed in Extended Data Table 1 and present-day individuals from the SGDP [47]) using all autosomal SNPs (~ 1.15 million) from our target set. For two replications of our admixture graph analyses, we restricted either to the subset of transversions (~ 280 K SNPs) or to the subset from panels 4 and 5 of the Affymetrix Human Origins array (ascertained as heterozygous in a San or Yoruba individual; ~ 260 K SNPs). For PCA (Extended Data Figure 1), we merged with a large set of present-day samples [21] and used all autosomal Human Origins SNPs (~ 593 K).

To test for possible contamination, we used contamMix [48] and ANGSD [49] to estimate rates of apparent heterozygosity in haploid genome regions (mtDNA and the X chromosome in males, respectively). Any samples with $> 5\%$ mtDNA mismatching or $> 2\%$ X contamination were excluded from further analyses, with the exception of Blätterhöhle individual Bla5, which was differentiated from all other samples with signs of mtDNA contamination by its substantially higher coverage on the nuclear genome ($\sim 5x$, all others $< 1x$, median $\sim 0.1x$; Supplementary Table 1), was comprised of data from six merged

libraries, and did not deviate noticeably from the other Blätterhöhle individuals in our analyses. We also removed samples identified as clear outliers in PCA or with significant population genetic differences between all sequencing data and genotypes called only from sequences displaying ancient DNA damage signatures. A total of 17 samples were excluded based on one of these criteria. For individual-level f -statistic analyses (Figure 2A–B), we restricted to samples with a maximum level of uncertainty, defined as a standard error of at most 7×10^{-4} for the statistic $f_4(\text{Mbuti, WHG; Anatolia, } X)$. This threshold (corresponding to an average coverage of approximately 0.05, or $\sim 60\text{K}$ SNPs hit at least once) was met by 87 of the 110 samples passing QC (and 49 of the 50 samples from the literature). We did not impose such a threshold for *ALDER* analyses, but because low coverage results in a weaker signal, only one of the 23 high-uncertainty individuals in our primary data set provided an *ALDER* date (as compared to 86 of the 128 low-uncertainty individuals).

Population assignments for analyses

In most cases, population groupings were used that correspond to archaeological culture assignments based on chronology, geography, and material culture traits. Occasionally, we merged populations that appeared similar genetically in order to increase power: we pooled samples from all phases and groups of the eastern Hungarian MN into a single ALPc population; merged six Sopot with eight Lengyel individuals for the western Hungarian TDLN; combined one Hunyadhalom (Middle CA from the Danube-Tisza interfluvium in central Hungary) with Lasinja; pooled four LBK samples from Stuttgart with the majority from farther to the northeast (primarily Halberstadt); and merged several cultures of the German MN into a single group. Other populations vary in their degrees of date and site heterogeneity, with Iberia MN the most homogeneous and Iberia EN and

CA among the least (Extended Data Table 1; Supplementary Table 1). For our main analyses, we excluded the Vinča and Tiszapolgár population groups because they lacked sufficient high-quality data.

We note that the designations EN, MN, LN, and CA have different meanings in different areas. For our study regions, each term generally refers to an earlier period in Hungary than in Germany and Spain (for example, ALPc and LBKT MN in Hungary are roughly contemporaneous with LBK and Iberia EN). In order to maintain agreement with the archaeological literature, we use the established definitions, with the appropriate word of caution that they should be treated separately in each region.

Sample dates

We report 44 newly obtained accelerator mass spectrometry (AMS) radiocarbon dates for Neolithic individuals (38 direct, 6 indirect), focusing on representative high-quality samples from each site and any samples with chronological uncertainty. These are combined with 57 radiocarbon dates from the literature [9, 10, 12, 22, 23, 35, 38, 39, 50]. We report the 95.4% calibrated confidence intervals (CI) from OxCal [51] version 4.2 with the IntCal13 calibration curve [52] in Extended Data Table 1. For use in *ALDER* analyses (Supplementary Information section 7), we use the mean and standard deviation of the calibrated date distributions; while the distributions are non-normal, we find that on average the mean plus or minus two standard deviations contains more than 95.4% of the probability density. For samples without direct radiocarbon dates but with dates from other samples or materials at the same site, we form a conservative 95.4% CI by taking the minimum and maximum bounds of any of the calibrated CIs from the site. Finally, for the remaining samples, we use plausible date ranges based on archaeological context; we assume independence across individuals but as a result take a conservative approach and

treat the assigned range as \pm one standard error (e.g., an estimated range of 4800–4500 BCE becomes 4650 ± 150 BCE).

Acknowledgments

We thank Iosif Lazaridis, Po-Ru Loh, Iain Mathieson, Iñigo Olalde, Nick Patterson, and Pontus Skoglund for helpful comments and suggestions; Johannes Krause for providing the Stuttgart sample for which we generated a new library in this study; and Bálint Havasi (Balaton Museum), György V. Székely (Katona József Museum), Csilla Farkas (Dobó István Museum), Borbála Nagy (Herman Ottó Museum), I. Pap, A. Kustár, T. Hajdu (Hungarian Natural History Museum), J. Ódor (Wosinsky Mór Museum), E. Nagy (Janus Pannonius Museum), P. Rácz (King St. Stephen Museum), L. Szathmáry (Debrecen University), N. Kalicz, V. Voicsek, O. Vajda-Kiss, V. Majerik, and I. Kővári for assistance with samples. This work was supported by the Australian Research Council (grant DP130102158; B.L. and W.H.), Hungarian National Research, Development and Innovation Office (K 119540; B.M.), German Research Foundation (AL 287-10-1; K.W.A.), FEDER and Ministry of Economy and Competitiveness of Spain (BFU2015-64699-P; C.L.-F.), National Science Foundation (HOMINID grant BCS-1032255; D.R.), National Institutes of Health (NIGMS grant GM100233; D.R.), and Howard Hughes Medical Institute (D.R.).

Author contributions

A.S.-N., J.B., E.B., K.W.A., C.L.-F., W.H., and D.R. designed and supervised the study. B.G.M., K.K., K.O., M.B., T.M., A.O., J.J., T.P., F.H., P.C., J.K., K.Se., A.A., P.R., J.R., J.P.B., S.F., G.S., Z.T., E.G.N., J.D., E.M., G.P., L.M., B.M., Z.B., J.F.-E., J.A.M.-

A., C.A.F., J.J.E., R.B., J.O., K.Sc., H.M., A.C., J.B., E.B., K.W.A., C.L.-F., and W.H. provided samples and assembled archaeological and anthropological information. A.S.-N., A.P., B.S., V.K., N.R., K.St., M.F., M.M., J.O., N.B., E.H., S.N., and B.L. performed laboratory work. M.L., A.S.-N., S.M., and D.R. analyzed genetic data. M.L., A.S.-N., and D.R. wrote the manuscript with input from all coauthors.

References

1. Ammerman, A. J. & Cavalli-Sforza, L. L. *The Neolithic transition and the genetics of populations in Europe* (Princeton, 1984).
2. Zvelebil, M. The agricultural transition and the origins of Neolithic society in Europe. *Documenta Praehistorica* **28**, 1–26 (2001).
3. Richards, M. The Neolithic invasion of Europe. *Ann. Rev. Anthropol.* 135–162 (2003).
4. Dupanloup, I., Bertorelle, G., Chikhi, L. & Barbujani, G. Estimating the impact of prehistoric admixture on the genome of Europeans. *Mol. Biol. Evol.* **21**, 1361–1372 (2004).
5. Currat, M. & Excoffier, L. The effect of the Neolithic expansion on European molecular diversity. *Proc. R. Soc. B* **272**, 679–688 (2005).
6. Bramanti, B. *et al.* Genetic discontinuity between local hunter-gatherers and Central Europe’s first farmers. *Science* **326**, 137–140 (2009).
7. Haak, W. *et al.* Ancient DNA from European early Neolithic farmers reveals their Near Eastern affinities. *PLoS Biol.* **8**, e1000536 (2010).
8. Skoglund, P. *et al.* Origins and genetic legacy of Neolithic farmers and hunter-gatherers in Europe. *Science* **336**, 466–469 (2012).
9. Lazaridis, I. *et al.* Ancient human genomes suggest three ancestral populations for present-day Europeans. *Nature* **513**, 409–413 (2014).
10. Haak, W. *et al.* Massive migration from the steppe was a source for Indo-European languages in Europe. *Nature* **522**, 207–211 (2015).
11. Günther, T. *et al.* Ancient genomes link early farmers from Atapuerca in Spain to modern-day Basques. *Proc. Natl. Acad. Sci. U. S. A.* **112**, 11917–11922 (2015).
12. Mathieson, I. *et al.* Genome-wide patterns of selection in 230 ancient Eurasians. *Nature* **528**, 499–503 (2015).

13. Hofmanová, Z. *et al.* Early farmers from across Europe directly descended from Neolithic Aegeans. *Proc. Natl. Acad. Sci. U. S. A.* 201523951 (2016).
14. Tringham, R. Southeastern Europe in the transition to agriculture in Europe: bridge, buffer or mosaic. In Price, T. D. (ed.) *Europe's First Farmers*, 19–56 (Cambridge, 2000).
15. Price, T. D. Lessons in the transition to agriculture. In Price, T. D. (ed.) *Europe's First Farmers*, 301–18 (Cambridge, 2000).
16. Vanmontfort, B. Forager–farmer connections in an ‘unoccupied’ land: First contact on the western edge of LBK territory. *J. Anthropol. Arch.* **27**, 149–160 (2008).
17. Keller, A. *et al.* New insights into the Tyrolean Iceman’s origin and phenotype as inferred by whole-genome sequencing. *Nat. Comm.* **3**, 698 (2012).
18. Bollongino, R. *et al.* 2000 years of parallel societies in Stone Age Central Europe. *Science* **342**, 479–481 (2013).
19. Skoglund, P. *et al.* Genomic diversity and admixture differs for Stone-Age Scandinavian foragers and farmers. *Science* **344**, 747–750 (2014).
20. Brandt, G. *et al.* Ancient DNA reveals key stages in the formation of Central European mitochondrial genetic diversity. *Science* **342**, 257–261 (2013).
21. Lazaridis, I. *et al.* Genomic insights into the origin of farming in the ancient Near East. *Nature* **536**, 419–424 (2016).
22. Gamba, C. *et al.* Genome flux and stasis in a five millennium transect of European prehistory. *Nat. Comm.* **5**, 5257 (2014).
23. Olalde, I. *et al.* A common genetic origin for early farmers from Mediterranean Cardial and Central European LBK cultures. *Mol. Biol. Evol.* **32**, 3132–3142 (2015).
24. Olalde, I. *et al.* Derived immune and ancestral pigmentation alleles in a 7,000-year-old Mesolithic European. *Nature* **507**, 225–228 (2014).
25. Fu, Q. *et al.* The genetic history of Ice Age Europe. *Nature* **534**, 200–205 (2016).

26. Patterson, N., Price, A. & Reich, D. Population structure and eigenanalysis. *PLoS Genet.* **2**, e190 (2006).
27. Jones, E. R. *et al.* Upper Palaeolithic genomes reveal deep roots of modern Eurasians. *Nat. Comm.* **6**, 8912 (2015).
28. Seguin-Orlando, A. *et al.* Genomic structure in Europeans dating back at least 36,200 years. *Science* **346**, 1113–1118 (2014).
29. Patterson, N. *et al.* Ancient admixture in human history. *Genetics* **192**, 1065–1093 (2012).
30. Loh, P.-R. *et al.* Inferring admixture histories of human populations using linkage disequilibrium. *Genetics* **193**, 1233–1254 (2013).
31. Fenner, J. Cross-cultural estimation of the human generation interval for use in genetics-based population divergence studies. *Am. J. Phys. Anthropol.* **128**, 415–423 (2005).
32. Moorjani, P. *et al.* A genetic method for dating ancient genomes provides a direct estimate of human generation interval in the last 45,000 years. *Proc. Natl. Acad. Sci. U. S. A.* 201514696 (2016).
33. Bánffy, E. Eastern, Central and Western Hungary – variations of Neolithisation models. *Documenta Praehistorica* **33**, 125–142 (2006).
34. Domboróczki, L., Kaczanowska, M. & Kozłowski, J. The Neolithic settlement at Tiszaszőlős-Domaháza-puszta and the question of the northern spread of the Körös Culture. *Atti Soc. Preist. Protost. Friuli-VG* **17**, 101–155 (2010).
35. Szécsényi-Nagy, A. *et al.* Tracing the genetic origin of Europe’s first farmers reveals insights into their social organization. *Proc. Royal Soc. B* **282**, 20150339 (2015).
36. Raczky, P. Historical context of the Late Copper Age Cemetery at Budakalász. In Bondár, M. & Raczky, P. (eds.) *The Copper Age Cemetery of Budakalász*, 475–485 (Pytheas, Budapest, 2009).

37. Martins, H. *et al.* Radiocarbon dating the beginning of the Neolithic in Iberia: New results, new problems. *J. Medit. Arch.* **28**, 105–131 (2015).
38. Jakucs, J. *et al.* Between the Vinča and Linearbandkeramik worlds: The diversity of practices and edentities in the 54th–53rd centuries cal BC in Southwest Hungary and beyond. *J. World Prehist.* **29**, 267–336 (2016).
39. Oross, K. *et al.* Midlife changes: The Sopot burial ground at Alsónyék. *Bericht der Römisch-Germanischen Kommission* **94**, 151–178 (2016).
40. Dabney, J. *et al.* Complete mitochondrial genome sequence of a Middle Pleistocene cave bear reconstructed from ultrashort DNA fragments. *Proc. Natl. Acad. Sci. U. S. A.* **110**, 15758–15763 (2013).
41. Korlević, P. *et al.* Reducing microbial and human contamination in DNA extractions from ancient bones and teeth. *BioTechniques* **59**, 87–93 (2015).
42. Rohland, N., Harney, E., Mallick, S., Nordenfelt, S. & Reich, D. Partial uracil–DNA–glycosylase treatment for screening of ancient DNA. *Phil. Trans. R. Soc. B* **370**, 20130624 (2015).
43. Meyer, M. *et al.* A mitochondrial genome sequence of a hominin from Sima de los Huesos. *Nature* **505**, 403–406 (2014).
44. Sawyer, S., Krause, J., Guschanski, K., Savolainen, V. & Pääbo, S. Temporal patterns of nucleotide misincorporations and DNA fragmentation in ancient DNA. *PloS one* **7**, e34131 (2012).
45. Andrews, R. M. *et al.* Reanalysis and revision of the Cambridge reference sequence for human mitochondrial DNA. *Nat. Genet.* **23**, 147 (1999).
46. Behar, D. M. *et al.* A “Copernican” reassessment of the human mitochondrial DNA tree from its root. *Am. J. Hum. Genet.* **90**, 675–684 (2012).
47. Mallick, S. *et al.* The Simons Genome Diversity Project: 300 genomes from 142 diverse populations. *Nature* **538**, 201–206 (2016).

48. Fu, Q. *et al.* DNA analysis of an early modern human from Tianyuan Cave, China. *Proc. Natl. Acad. Sci. U. S. A.* **110**, 2223–2227 (2013).
49. Korneliussen, T. S., Albrechtsen, A. & Nielsen, R. ANGSD: analysis of next generation sequencing data. *BMC Bioinformatics* **15**, 356 (2014).
50. Oross, K. *et al.* The early days of Neolithic Alsónyék: the Starčevo occupation. *Bericht der Römisch-Germanischen Kommission* **94**, 93–121 (2016).
51. Ramsey, C. B. & Lee, S. Recent and planned developments of the program OxCal. *Radiocarbon* **55**, 720–730 (2013).
52. Reimer, P. J. *et al.* Intcal13 and marine13 radiocarbon age calibration curves 0–50,000 years cal bp. *Radiocarbon* **55**, 1869–1887 (2013).

Extended Data Table 1. Descriptive statistics, background information, and admixture parameters for Neolithic individuals in the study.

ID	Population	Site	Lat.	Long.	Date	Sex	Mt Hap	Y Hap	Cov.	HG%	ALD	Ref.
GEN68	Körös	Törökszentmiklós road 4 site 3	47.2	20.4	5706–5541	F	K1a	..	2.46	-0.09±1.6	±	
HUNG276, KO2	Körös	Tiszaszőlős-Domaháza	47.3	21.5	5713–5566	F	K1a	..	0.91	-1.51±1.6	±	[12, 22]
BAM17b	Starčevo	Alsónyék-Bátaszék, Mérnöki telep	46.2	18.7	5832–5667	M	T1a2	H2	1.47	7.85±1.7	4.5±1.9	
BAM25	Starčevo	Alsónyék-Bátaszék, Mérnöki telep	46.2	18.7	5702–5536	M	N1a1a1	H2	0.22	1.63±1.9	±	[10, 12]
BAM4a	Starčevo	Alsónyék-Bátaszék, Mérnöki telep	46.2	18.7	5641–5547	M	K1a4	G2a2a1	0.20	3.43±2.0	±	
LGCS1a	Starčevo	Lánycsók	46.0	18.6	5800–5500	M	W5	G2a2b2b1a	0.77	-0.64±1.7	±	
BAL25b	LBKT	Bátaszék-Lajvér	46.2	18.7	5208–4948	M	K1b1a	G2a2a1	2.77	0.06±1.5	±	
BOVO1b	LBKT	Bölcske-Gyűrűsvölgy	46.7	19.0	5300–4900	F	H	..	0.01	11.1±6.4	±	
BUD4a	LBKT	Budakeszi-Szőlőskert	47.5	18.9	5300–4900	M	T1a	G2a2b2a	0.17	6.80±2.3	36±6.2	
BUD9a	LBKT	Budakeszi-Szőlőskert	47.5	18.9	5300–4900	F	U2	..	1.10	1.89±1.6	±	
GEN18	LBKT	Alsónyék, site 11	46.2	18.7	5309–5074	M	T2c1	G2a2b2b1	1.48	2.69±1.5	35±12	
KON3	LBKT	Enese elkerülő, Kóny, Proletár-dűlő, M85, Site 2	47.6	17.4	5300–4900	F	T2b	..	0.03	2.82±4.1	±	
SZE4	LBKT	Szemely-Hegyes	46.4	18.7	5207–4944	F	N1a1a1a3	..	0.07	1.90±3.1	±	[10, 12]
CEG07b	ALPc	Cegléd, site 4/1	47.2	19.9	5300–4900	M	J2b1	G2a2b2a	0.30	11.5±2.0	±	
CEG08b	ALPc	Cegléd, site 4/1	47.2	19.9	5300–4900	F	J1c1	..	0.19	11.2±2.2	23±3.1	
EBSA2a	ALPc	Ebes-Sajtgár	47.5	21.5	5300–4900	F	K1a	..	0.05	16.4±3.1	±	
EBVO5a	ALPc	Ebes-Zsongvölgy	47.5	21.5	5300–4900	M	V1a	CT	0.04	9.36±3.3	±	
HAE10a	ALPc	Hajdúnánás-Eszlári út	47.9	21.4	5221–5000	M	J2b1	I	0.29	11.0±1.8	±	
HAE7a	ALPc	Hajdúnánás-Eszlári út	47.9	21.4	5302–5057	M	K1a	I2	1.57	9.26±1.8	6.2±5.7	
HELI11a	ALPc	Hejőkürt-Lidl	47.9	21.0	5209–4912	M	N1a1a1	I2a2a1b	0.99	6.08±1.8	14±2.0	
HELI2a	ALPc	Hejőkürt-Lidl	47.9	21.0	5300–4900	M	U8b1b	I	0.09	7.48±2.6	±	
HUNG302, NE2	ALPc	Debrecen Tocopart Erdoalja	47.5	21.6	5291–5056	F	H	..	4.88	11.1±1.7	±	[12, 22]
HUNG372, NE5	ALPc	Kompolt-Kígyóvár	47.2	20.8	5295–4950	M	J1c1	C1a2	4.25	7.56±1.7	±	[12, 22]
HUNG86, NE3	ALPc	Garadna-Elkerülő út site 2	48.5	21.2	5281–5026	F	X2b-T226C	..	3.32	12.2±1.7	18±3.1	[12, 22]
MEMO24b	ALPc	Mezőkövesd-Mocsolyás	47.8	20.6	5500–5300	M	U8b1b	CT	0.04	11.8±3.3	26±12	
MEMO2b	ALPc	Mezőkövesd-Mocsolyás	47.8	20.6	5500–5300	F	K1a1	..	2.28	9.10±1.7	24±5.2	
MEMO7a	ALPc	Mezőkövesd-Mocsolyás	47.8	20.6	5500–5300	F	HV	..	0.26	1.66±2.0	13±6.1	
PF325, NE1	ALPc	Polgár-Ferenci-hát	47.9	21.2	5306–5071	F	U5b2c	..	1.52	8.21±1.8	11±3.9	[12, 22]
PF839/1198, NE4	ALPc	Polgár-Ferenci-hát	47.9	21.2	5211–5011	F	J1c5	..	3.49	10.1±1.7	25±9.9	[12, 22]
POPI5a	ALPc	Polgár-Piócás	47.9	21.1	5300–4900	M	K1a1	I2a2a	0.31	9.87±2.0	11±3.7	
PULE1.18a	ALPc	Pusztataskony-Ledence	47.5	20.5	5300–4900	F	T2c1d1	..	0.29	10.8±1.9	±	
PULE1.23a	ALPc	Pusztataskony-Ledence	47.5	20.5	5300–4900	F	H1e	..	0.17	9.63±2.2	11±3.4	
TISO13a	ALPc	Tiszadob-Ökenéz	48.0	21.2	5208–4942	M	J1c2	I2a2a	1.21	13.0±1.7	22±7.6	
TISO1b	ALPc	Tiszadob-Ökenéz	48.0	21.2	5300–4900	M	H7	I2a2a1b1	0.11	7.32±2.5	29±13	
TISO3a	ALPc	Tiszadob-Ökenéz	48.0	21.2	5300–4900	F	U5b2b1a	..	0.27	12.3±2.1	8.4±5.2	
SEKU10a	Vinča	Szederkény-Kukorica-dűlő	45.6	18.3	5320–5080	M	K2a	G2a2b2a1a	0.24	2.30±2.0	±	
SEKU6a	Vinča	Szederkény-Kukorica-dűlő	45.6	18.3	5321–5081	F	H26	..	1.15	9.27±1.7	9.1±9.4	
VEGI17a	Vinča	Versend-Gilencsa	45.6	18.3	5400–5000	F	U2	..	0.01	-6.22±5.6	±	
VEGI3a	Vinča	Versend-Gilencsa	45.6	18.3	5400–5000	M	T2b	H2	0.41	0.54±1.8	±	
Gorzs18	Tisza	Hódmezővásárhely-Gorzsa	46.4	20.4	5000–4500	M	U5b2c	I2a1	6.87	7.86±1.7	13±4.2	
Gorzs4	Tisza	Hódmezővásárhely-Gorzsa	46.4	20.4	5000–4500	F	T1a	..	0.06	11.4±3.1	23±11	
KOKE3a	Tisza	Hódmezővásárhely-Kökénydomb Vörös tanya	46.4	20.2	5000–4500	M	K1b1	I	0.06	13.9±3.2	±	
PULE1.24	Tisza	Pusztataskony-Ledence	47.5	20.5	5000–4500	F	K1a4	..	0.40	10.5±1.9	18±7.1	
VSM3a	Tisza	Vesztő-Mágó	46.9	21.2	5000–4500	M	H26	G2a	0.09	7.00±2.6	±	
ALE14a	TDLN	Alsónyék-Elkerülő site 2	46.2	18.7	5030–4848	M	U8b1b	G2a	0.05	-1.12±3.2	±	
ALE4a	TDLN	Alsónyék-Elkerülő site 2	46.2	18.7	5016–4838	M	T2c1	F	0.03	10.7±3.6	±	
BAL3a	TDLN	Bátaszék-Lajvér	46.2	18.7	4800–4500	M	T2f	H1b1	0.91	6.97±1.7	22±9.1	
CSAT19a	TDLN	Csabdi-Télizöldes	47.5	18.6	4800–4500	M	H	H	0.52	5.89±1.8	34±9.6	
CSAT25a	TDLN	Csabdi-Télizöldes	47.5	18.6	4826–4602	M	T2b	I2	0.43	13.7±1.9	26±8.1	
FAGA1a	TDLN	Fajsz-Garadomb	46.4	18.9	5100–4750	M	HV0a	I	0.09	5.13±2.4	±	
FAGA2a	TDLN	Fajsz-Garadomb	46.4	18.9	5195–4842	F	H	..	0.49	12.1±1.8	14±4.1	
FEB3a	TDLN	Felső-Bárókert	47.0	18.0	4800–4500	M	H44	J2a	0.16	6.38±2.1	±	
HUNG347, NE7	TDLN	Apc-Berekalja	47.2	19.8	4491–4357	M	N1a1a1a	I	4.85	10.7±1.6	19±3.1	[12, 22]
SZE45a	TDLN	Szemely-Hegyes	46.0	18.3	4904–4709	M	K1b1a	G	0.01	10.9±6.6	±	
SZE47b	TDLN	Szemely-Hegyes	46.0	18.3	4930–4715	F	K1a	..	0.52	3.48±1.7	±	
VEJ12a	TDLN	Veszprém Jutasi út	47.1	17.9	4800–4500	M	U8b1a2b	H	0.10	6.24±2.3	±	
VEJ2a	TDLN	Veszprém Jutasi út	47.1	17.9	4800–4500	M	T2b	C	0.34	5.69±1.8	±	
VEJ5a	TDLN	Veszprém Jutasi út	47.1	17.9	4800–4500	M	J1c2	G2a2a1	0.62	7.87±1.8	15±2.9	
GEN67	Tiszapolgár	Törökszentmiklós road 4 site 3	47.2	20.4	4444–4257	M	H1	I2a2a1b	2.28	13.1±1.7	50±15	
PULE1.10a	Tiszapolgár	Pusztataskony-Ledence	47.5	20.5	4500–4000	M	T2c1	I2a	0.28	9.14±2.0	±	
PULE1.13a	Tiszapolgár	Pusztataskony-Ledence	47.5	20.5	4500–4000	M	T2c1	G2a2b2a1a1c1a	0.38	10.4±1.9	±	
PULE1.9a	Tiszapolgár	Pusztataskony-Ledence	47.5	20.5	4500–4000	M	H26	G2a2b	0.11	11.7±2.4	±	
GEN100	Lásinja	Alsónyék, site 11	46.2	18.7	4300–3900	F	T2b	..	1.81	9.62±1.6	45±11	
GEN49	Lásinja	Nemesnádudvar-Papföld	46.3	19.1	4228–3963	M	T2b23	CT	0.97	12.9±1.8	27±6.8	
KEFP2a	Lásinja	Keszthely-Fenékpuszta	46.7	17.2	4300–3900	F	J2b1a	..	0.74	9.23±1.7	21±5.4	
KON2a	Lásinja	Enese elkerülő, Kóny, Proletár-dűlő, M85, Site 2	47.6	17.4	4333–4072	F	K2a	..	2.13	10.4±1.7	21±6.4	
M6-116.12a	Lásinja	Lánycsók, Csata-alja	46.0	18.6	4232–4046	F	T2f8a	..	0.64	9.79±1.7	29±11	
VEJ9a	Lásinja	Veszprém Jutasi út	47.1	17.9	4339–4237	M	H40	CT	0.05	8.93±3.2	±	
GEN60	Protoboleráz	Abony, Turjános-dűlő	47.2	20.0	3909–3651	M	H	G2a2b2a	1.88	14.2±1.6	37±8.8	
GEN61	Protoboleráz	Abony, Turjános-dűlő	47.2	20.0	3800–3600	M	J1c	I2c	0.76	10.9±1.7	65±14	
GEN62	Protoboleráz	Abony, Turjános-dűlő	47.2	20.0	3800–3600	F	N1a1a1a3	..	4.81	8.10±1.6	37±9.6	
GEN63	Protoboleráz	Abony, Turjános-dűlő	47.2	20.0	3762–3636	M	U5a1c1	I2c	1.92	12.0±1.7	34±8.1	
GEN12a	Baden	Budakalász-Luppa csárda	47.6	19.0	3300–2850	M	H26a	G2a2b2a1a1b1	1.98	14.0±1.7	34±7.2	
GEN13a	Baden	Budakalász-Luppa csárda	47.6	19.0	3300–2850	M	HV	G2a2b2a1a	2.65	11.4±1.6	27±6.6	
GEN15a	Baden	Budakalász-Luppa csárda	47.6	19.0	3367–3103	M	J2a1a1	G2a2b2a1a1c1a	1.66	10.9±1.7	22±9.2	
GEN16a	Baden	Alsónémedi	47.3	19.2	3300–2850	F	T2b	..	4.30	13.0±1.6	38±16	
GEN17a	Baden	Alsónémedi	47.3	19.2	3359–3098	M	U5b3f	G2a2a	0.82	10.9±1.7	21±6.3	
GEN21	Baden	Balatonlelle-Felső-Gamász	46.8	17.7	3600–2850	M	K1a	I2a1	0.67	12.4±1.7	±	
GEN22	Baden	Balatonlelle-Felső-Gamász	46.8	17.7	3600–2850	M	U5a1	I2a1a1	2.31	14.7±1.7	25±6.6	
GEN55	Baden	Vámosgyörk	47.7	19.9	3600–2850	F	T2c2	..	0.81	13.2±1.8	22±6.7	
HUNG353, CO1	Baden	Apc-Berekalja	47.2	19.8	3315–2923	F	H	..	4.56	15.3±1.7	37±15	[12, 22]
Vors1	Baden	Vörs	46.7	17.3	3300–2850	F	T2f	..	0.03	4.52±4.2	±	

Continued on next page

Extended Data Table 1 – continued from previous page

ID	Population	Site	Lat.	Long.	Date	Sex	Mt Hap	Y Hap	Cov.	HG%	ALD	Ref.
HAL03a	LBK	Halberstadt-Sonntagsfeld	51.9	11.0	5295–5057	F	T2b	..	0.01	-5.19±6.8	±	
HAL07a	LBK	Halberstadt-Sonntagsfeld	51.9	11.0	5212–4992	F	N1a1b	..	0.05	1.74±3.2	±	
HAL15a	LBK	Halberstadt-Sonntagsfeld	51.9	11.0	5199–4857	M	N1a1a3	G2	0.02	5.32±5.0	±	
HAL17b	LBK	Halberstadt-Sonntagsfeld	51.9	11.0	5500–4850	F	V1	..	0.02	9.32±4.3	±	
HAL18a	LBK	Halberstadt-Sonntagsfeld	51.9	11.0	5500–4850	F	K2a	..	0.02	0.27±4.7	±	
HAL19	LBK	Halberstadt-Sonntagsfeld	51.9	11.0	5500–4850	F	K1a2	..	0.86	7.18±1.7	17±5.6	[12]*
HAL2	LBK	Halberstadt-Sonntagsfeld	51.9	11.0	5211–4963	M	N1a1a1a2	G2a2a1	0.76	1.93±1.7	10±2.3	[10,12]*
HAL20b	LBK	Halberstadt-Sonntagsfeld	51.9	11.0	5500–4850	M	K1a2	G2a2a	0.06	2.56±3.1	±	
HAL21a	LBK	Halberstadt-Sonntagsfeld	51.9	11.0	5500–4850	M	T2b	G2a2a	0.01	-4.46±5.9	±	
HAL22b	LBK	Halberstadt-Sonntagsfeld	51.9	11.0	5500–4850	F	T2b	..	0.02	-7.80±4.8	±	
HAL24	LBK	Halberstadt-Sonntagsfeld	51.9	11.0	5201–4850	M	X2d1	G2a2a1	0.42	6.47±1.8	±	[10,12]*
HAL25	LBK	Halberstadt-Sonntagsfeld	51.9	11.0	5210–5002	M	K1a	G2a2a1	0.49	2.61±1.7	17±7.5	[10,12]*
HAL27a	LBK	Halberstadt-Sonntagsfeld	51.9	11.0	5500–4850	M	N1a1a3	G2a2a	0.05	3.88±3.0	±	
HAL31a	LBK	Halberstadt-Sonntagsfeld	51.9	11.0	5295–5057	F	K1c	..	0.12	4.59±2.3	10±3.1	
HAL32b	LBK	Halberstadt-Sonntagsfeld	51.9	11.0	5500–4850	F	H26	..	0.23	3.37±2.0	±	
HAL34	LBK	Halberstadt-Sonntagsfeld	51.9	11.0	5219–5021	F	N1a1a1	..	0.25	5.69±2.0	10±4.0	[10,12]*
HAL35b	LBK	Halberstadt-Sonntagsfeld	51.9	11.0	5500–4850	F	J1c	..	0.10	3.98±2.4	±	
HAL38a	LBK	Halberstadt-Sonntagsfeld	51.9	11.0	5500–4850	F	V1	..	0.29	1.12±1.9	±	
HAL39b	LBK	Halberstadt-Sonntagsfeld	51.9	11.0	5210–5002	M	H1e	G2a2a1	0.08	4.01±2.7	±	
HAL4	LBK	Halberstadt-Sonntagsfeld	51.9	11.0	5202–4852	F	N1a1a1a	..	6.92	6.62±1.6	18±5.8	[10,12]*
HAL40a	LBK	Halberstadt-Sonntagsfeld	51.9	11.0	5500–4850	F	T2b	..	0.17	2.53±2.1	±	
HAL5	LBK	Halberstadt-Sonntagsfeld	51.9	11.0	5211–4991	F	T2c1	..	2.23	3.01±1.6	10±6.9	[10,12]*
KAR16A	LBK	Karsdorf	51.3	11.7	5500–4850	M	H46b	T1a	0.09	0.29±2.7	13±5.1	[12]
KAR6	LBK	Karsdorf	51.3	11.7	5217–5041	M	H1/H1a1b	CT	0.10	5.85±2.6	±	[10,12]
LBK1976	LBK	Viesenhäuser Hof	48.8	9.2	5500–4850	F	T2e	..	0.44	3.50±1.7	18±4.4	[10,12]
LBK1992	LBK	Viesenhäuser Hof	48.8	9.2	5500–4850	F	T2b	..	2.66	5.75±1.6	12±4.3	[10,12]
LBK2155	LBK	Viesenhäuser Hof	48.8	9.2	5500–4850	F	T2b	..	3.63	4.89±1.5	13±4.4	[10,12]
Stuttgart	LBK	Viesenhäuser Hof	48.8	9.2	5310–5076	F	T2c1b	..	9.65	3.04±1.6	22±8.1	[9]*
UWS4	LBK	Unterwiederstedt	51.7	11.5	5223–5021	F	J1c17	..	18.6	5.76±1.6	13±14	[10,12]
ESP30	GermanyMN	Esperstedt	51.4	11.7	3970–3710	M	H1e1a	I	0.09	22.2±2.7	±	[10,12]
HAL13a	GermanyMN	Halberstadt-Sonntagsfeld	51.9	11.0	4600–4300	F	V1a	..	0.11	9.14±2.4	13±4.3	
QLB15D	GermanyMN	Quedlinburg	51.8	11.1	3654–3527	M	HV	R	0.16	21.1±2.2	36±8.7	[10,12]
QLB18A	GermanyMN	Quedlinburg	51.8	11.1	3640–3376	F	T2e1	..	0.41	19.8±1.8	23±4.9	[10,12]
SALZ3B	GermanyMN	Salzmünde-Schiebzig	51.5	11.8	3400–3025	M	U3a1	G2a2a1	0.09	15.1±2.7	±	[12]
SALZ57A	GermanyMN	Salzmünde-Schiebzig	51.5	11.8	3345–3097	F	H3	..	0.02	25.3±4.5	±	
SALZ77A	GermanyMN	Salzmünde-Schiebzig	51.5	11.8	3400–3025	M	H3	IJK (x J)	0.02	21.6±5.1	±	
Bla16	Blätterhöhle	Blätterhöhle Cave	51.4	7.6	3958–3344	M	U5b2a2	R1b1	0.80	39.9±2.0	15±5.8	
Bla28	Blätterhöhle	Blätterhöhle Cave	51.4	7.6	3337–3024	M	J1c1b1	R1	0.10	52.5±2.7	11±4.5	
Bla5	Blätterhöhle	Blätterhöhle Cave	51.4	7.6	3704–3117	F	H5	..	5.07	41.6±1.9	24±4.7	
Bla8	Blätterhöhle	Blätterhöhle Cave	51.4	7.6	4038–3532	M	U5b2b2	I2a1	4.58	73.4±2.0	12±2.9	
CB13	Iberia EN	Cova Bonica	41.4	1.9	5469–5327	F	K1a2a	..	0.98	10.1±1.8	17±3.5	[23]
E-06-Ind1	Iberia EN	El Prado de Pancorbo	42.6	-3.1	4827–4692	F	K1a4a1	..	0.47	8.82±1.9	17±2.3	
E-14-Ind2	Iberia EN	El Prado de Pancorbo	42.6	-3.1	5216–5031	F	H1	..	0.38	7.60±1.8	19±2.8	
Troc1	Iberia EN	Els Trocs	42.5	0.5	5311–5218	F	J1c3	..	0.69	7.23±1.8	12±9.0	[10,12]
Troc3	Iberia EN	Els Trocs	42.5	0.5	5294–5066	M	T2c1d/T2c1d2	R1b1a2	1.31	10.0±1.8	49±22	[10,12]
Troc5	Iberia EN	Els Trocs	42.5	0.5	5310–5078	M	N1a1a1	I2a1b1	13.8	6.91±1.6	6.8±2.8	[10,12]
Troc7	Iberia EN	Els Trocs	42.5	0.5	5303–5075	F	V	..	1.57	11.2±1.7	18±4.8	[10,12]
Mina18	Iberia MN	La Mina	41.3	-2.3	3893–3661	F	U5b1	..	13.6	23.1±1.8	42±18	[10,12]
Mina3	Iberia MN	La Mina	41.3	-2.3	3900–3600	M	K1a1b1	H2	0.38	19.7±1.9	80±20	[10,12]
Mina4	Iberia MN	La Mina	41.3	-2.3	3900–3600	M	H1	I2a2a1b2	3.95	22.8±1.9	25±6.3	[10,12]
Mina6	Iberia MN	La Mina	41.3	-2.3	3900–3600	F	K1b1a1	..	1.36	19.1±1.7	46±8.1	[10,12]
1.-K11	Iberia CA	La Chabola de la Hechicera	42.6	-2.6	3263–2903	M	X2b	I2a2	0.18	28.1±2.1	67±25	
3.-K11	Iberia CA	La Chabola de la Hechicera	42.6	-2.6	3627–3363	F	J2a1a1	..	0.12	24.7±2.5	30±12	
5.-K18	Iberia CA	La Chabola de la Hechicera	42.6	-2.6	3090–2894	M	J1c1	I2a2	0.10	18.7±2.5	43±11	
ES.1/4	Iberia CA	El Sotillo	42.6	-2.6	2571–2347	M	H3	I	0.07	25.6±2.8	±	
ES-6G-110	Iberia CA	El Sotillo	42.6	-2.6	2916–2714	M	H3	I2a2a	0.05	25.7±3.2	±	
Inventario0/4	Iberia CA	El Sotillo	42.6	-2.6	2481–2212	M	X2b	I2a2a	0.12	30.0±2.5	56±23	
LHUE11J.5	Iberia CA	Alto de la Huesera	42.6	-2.6	3092–2877	F	U5b1	..	1.19	27.0±1.9	40±9.7	
LHUE2010.10	Iberia CA	Alto de la Huesera	42.6	-2.6	3014–2891	F	J1c1	..	0.11	25.5±2.5	64±13	
LHUE2010.11	Iberia CA	Alto de la Huesera	42.6	-2.6	3092–2918	M	V	G2a2a	0.32	31.5±2.0	±	
LHUE2014.11J	Iberia CA	Alto de la Huesera	42.6	-2.6	3100–2850	F	U5b2b	..	0.06	26.6±3.0	±	
LY.II.A.10.15066	Iberia CA	Las Yurdinas II	42.6	-2.7	3350–2750	M	U5b2b3a	I2a2a	1.93	30.4±1.8	±	
LY.II.A.10.15067	Iberia CA	Las Yurdinas II	42.6	-2.7	3350–2750	F	J2a1a1	..	0.30	24.1±2.0	±	
LY.II.A.10.15068	Iberia CA	Las Yurdinas II	42.6	-2.7	3350–2750	F	K1a4a1a	..	0.39	29.5±2.0	28±10	
LY.II.A.10.15069	Iberia CA	Las Yurdinas II	42.6	-2.7	3354–2943	F	J1c3	..	4.24	25.4±1.7	29±15	
MIR1	Iberia CA	El Mirador Cave	42.3	-3.5	2900–2346	F	K1a	..	0.24	24.5±2.1	±	[12]
MIR13	Iberia CA	El Mirador Cave	42.3	-3.5	2900–2346	F	H3c3	..	0.10	28.1±2.4	±	[12]
MIR14	Iberia CA	El Mirador Cave	42.3	-3.5	2568–2346	M	H3	I2a2a	0.94	23.5±1.8	57±16	[12]
MIR17	Iberia CA	El Mirador Cave	42.3	-3.5	2900–2346	F	J1c1	..	0.22	23.8±2.2	±	[12]
MIR18	Iberia CA	El Mirador Cave	42.3	-3.5	2865–2575	F	H1t	..	1.58	20.2±1.6	43±17	[12]
MIR19	Iberia CA	El Mirador Cave	42.3	-3.5	2900–2346	M	H3	I	0.06	22.1±3.1	±	[12]
MIR2	Iberia CA	El Mirador Cave	42.3	-3.5	2857–2496	F	K1b1a1	..	0.98	22.9±1.8	56±9.0	[12]
MIR21	Iberia CA	El Mirador Cave	42.3	-3.5	2900–2346	M	H3	I	0.11	25.0±2.4	55±17	[12]
MIR22	Iberia CA	El Mirador Cave	42.3	-3.5	2900–2346	F	K1a2a	..	2.79	22.9±1.7	62±10	[12]
MIR24	Iberia CA	El Mirador Cave	42.3	-3.5	2900–2346	M	J2b1a3	G2a2b2b	0.06	20.3±3	±	[12]
MIR25	Iberia CA	El Mirador Cave	42.3	-3.5	2900–2346	M	U3a1	I2a1a1	0.73	25.5±1.7	±	[12]
MIR5, MIR6	Iberia CA	El Mirador Cave	42.3	-3.5	2900–2679	M	X2b	C1a2	10.4	21.0±1.7	107±41	[12]

Cov: average coverage per SNP. HG%: inferred percentage of hunter-gatherer ancestry (mean ± standard error). ALD: inferred date of admixture (generations in the past; mean ± standard error). Ref: reference for published data; if blank, newly published sample in this study (asterisk denotes a published individual with new sequencing data added). Radiocarbon dates are in normal text, while dates estimated from archaeological context are in italics. Further information can be found in Supplementary Table 1.

Extended Data Table 2. Admixture graph results for Neolithic populations

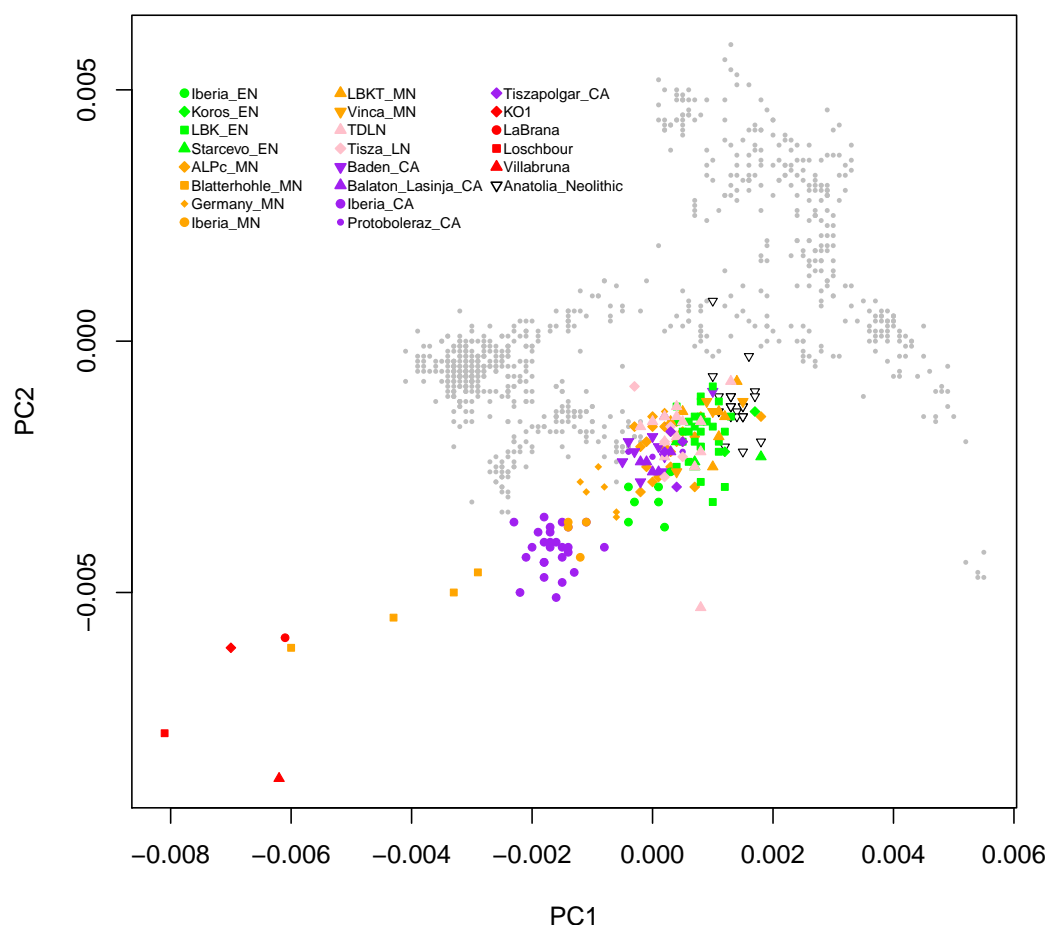
Neolithic pop	Main scaffold		Alternative scaffold	
	HG ancestry	WHG affinity	HG ancestry	WHG affinity
Körös EN	$0.0 \pm 1.2\%$		$0.0 \pm 1.2\%$	
Starčevo EN	$2.3 \pm 1.1\%$	K/V	$2.3 \pm 1.1\%$	V
ALPc MN	$8.8 \pm 0.6\%$	K* + V	$9.5 \pm 0.6\%$	K* + V
LBKT MN	$0.8 \pm 0.9\%$	V*	$0.5 \pm 0.9\%$	V
Tisza LN	$8.4 \pm 1.3\%$	K/V	$9.8 \pm 1.3\%$	K/V + E
TDLN	$8.2 \pm 0.7\%$	K/V*	$8.4 \pm 0.7\%$	K*
Lasinja CA	$10.7 \pm 0.9\%$	K/V*	$10.6 \pm 0.9\%$	K/V*
Protoboleráz CA	$12.7 \pm 0.9\%$	K/V*	$12.5 \pm 0.9\%$	K/V
Baden CA	$13.0 \pm 0.7\%$	K/V*	$13.4 \pm 0.7\%$	K*
LBK EN	$4.2 \pm 0.6\%$	K + LO	$5.0 \pm 0.6\%$	K*
Germany MN	$17.0 \pm 1.1\%$	LO*	$18.3 \pm 1.1\%$	LO + K
Blätterhöhle MN	$53.0 \pm 1.3\%$	LO* + K/V*	$54.0 \pm 1.3\%$	LO* + K*
Iberia EN	$10.0 \pm 0.8\%$	LB*	$10.4 \pm 0.8\%$	LB*
Iberia MN	$23.3 \pm 1.1\%$	LB* + LO	$24.8 \pm 1.1\%$	LB* + LO
Iberia CA	$26.8 \pm 0.7\%$	LB* + LO/K/V*	$27.6 \pm 0.7\%$	LB* + V*

Hunter-gatherer ancestry in Neolithic populations as inferred from admixture graph analyses. Shown are the inferred ancestry proportions for the best-fitting FEF+WHG model, along with the WHG individual(s) inferred to be related to the hunter-gatherer sources, with * denoting statistical significance (Methods). The two sets of results are for the primary scaffold model (Extended Data Figure 3) and an alternative admixture graph scaffold including EHG (Figure S6.1). E: EHG; K: KO1; LB: La Braña 1; LO: Loschbour; V: Villabruna; (LO)/K/V: either KO1 or Villabruna (or Loschbour).

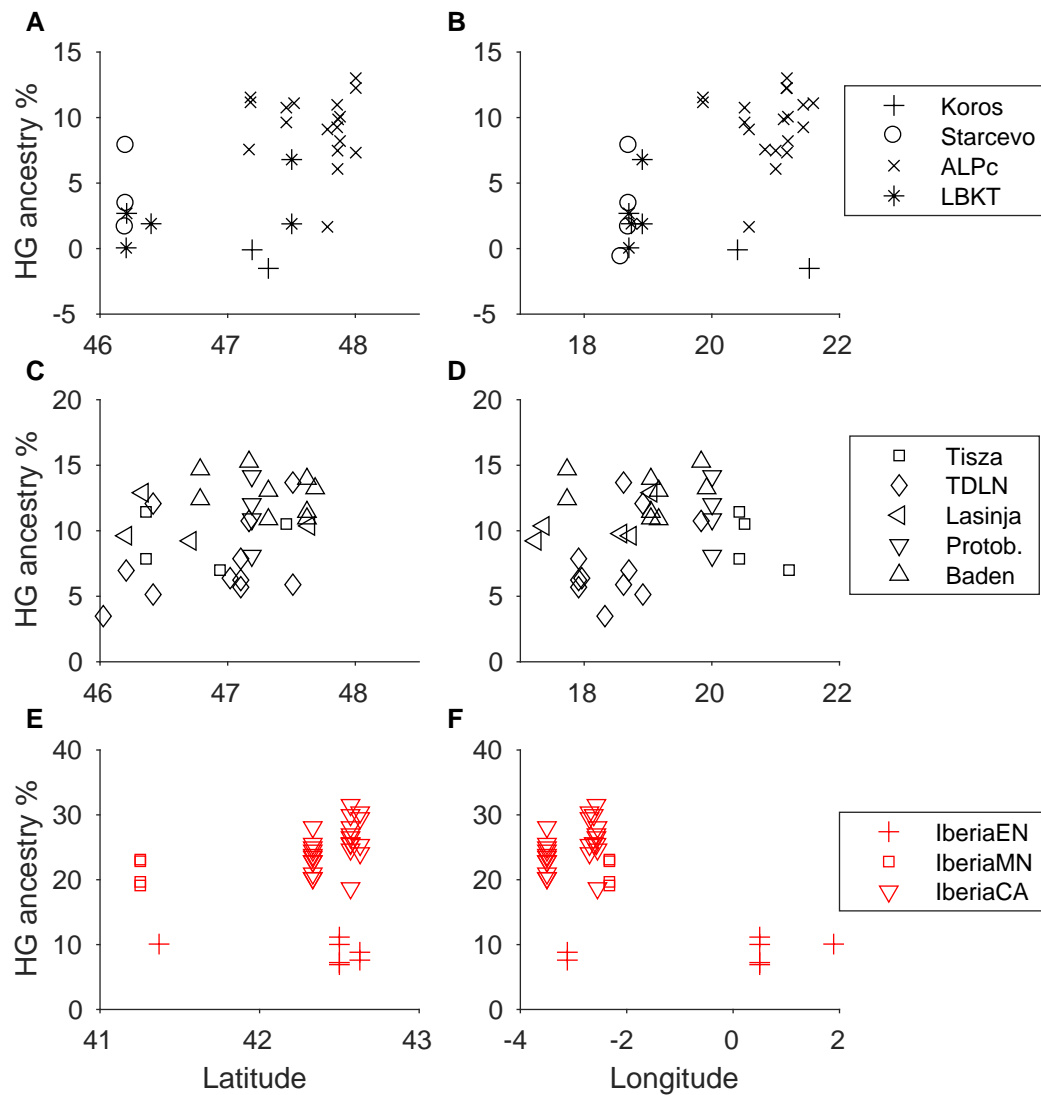
Extended Data Table 3. Average dates of admixture for Neolithic populations

Population	Individual-based	Group-based	Average sample date (BCE)
Körös EN			5633 \pm 28
Starčevo EN	4.5 \pm 1.9	2.9 \pm 1.6	5738 \pm 35
ALPc MN	18.7 \pm 2.3	16.4 \pm 2.6	5173 \pm 32
LBKT MN	35.5 \pm 7.1	46.4 \pm 17.7	5154 \pm 116
Tisza LN	18.2 \pm 6.6	12.7 \pm 3.1	4750 \pm 145
TDLN	21.6 \pm 3.0	19.0 \pm 3.8	4640 \pm 38
Lasinja CA	29.3 \pm 5.2	23.0 \pm 4.1	4123 \pm 59
Protoboleráz CA	44.3 \pm 6.5	19.8 \pm 5.3	3705 \pm 39
Baden CA	28.6 \pm 4.7	26.3 \pm 6.2	3142 \pm 74
LBK EN	14.3 \pm 2.5	13.9 \pm 4.7	5130 \pm 40
Germany MN	26.2 \pm 4.4	55.0 \pm 41.2	3719 \pm 46
Blätterhöhle MN	18.5 \pm 4.2	11.3 \pm 4.3	3581 \pm 86
Iberia EN	19.4 \pm 2.3	17.5 \pm 5.9	5107 \pm 20
Iberia MN	49.8 \pm 7.7	40.0 \pm 7.0	3749 \pm 74
Iberia CA	54.0 \pm 7.1	58.0 \pm 8.6	2814 \pm 27

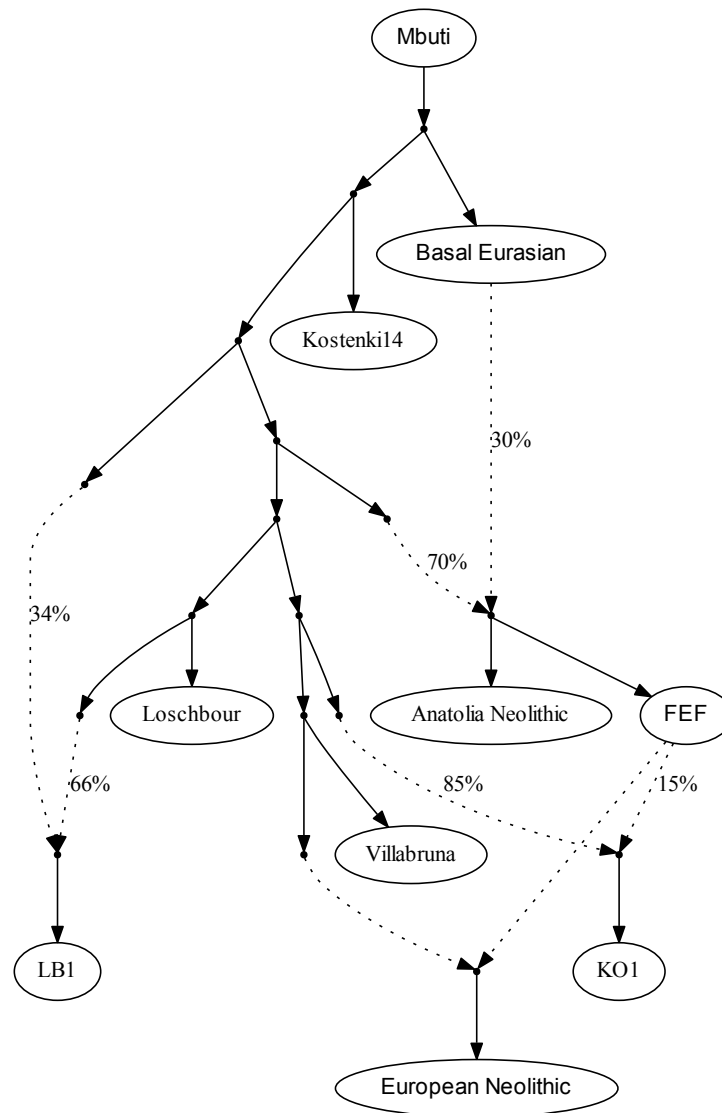
Dates of admixture (in generations in the past) as inferred from *ALDER* through two different methods. On the left are the average individual-level dates used in our main analyses, and on the right are direct estimates for population groups. By default, for group-level estimates, we used all individuals that yielded a date in our standard *ALDER* procedure, but because of missing data, for some populations we used a subset of individuals (typically those with highest coverage): Starčevo (BAM4a, BAM17b, and LGCS1a; we note that in this case only BAM17b had an *ALDER* signal individually), ALPc (NE3, NE1, NE4, TISO13a, HELI11a, MEMO2b, and HAJE7a), Tisza (Gorzsai18 and PULE1.24), Baden (GEN22, GEN55, CO1, GEN12a, GEN13a, GEN15a, and GEN17a), LBK (Stuttgart, LBK1992, HAL5, HAL4, HAL2, and HAL19), and Iberia CA (MIR14, MIR2, MIR18, MIR22, LY.II.A.10.15069, LHUE11J.5, and LY.II.A.10.15066). For Iberia MN, we used a fitting start point of 0.8 cM instead of the program-inferred minimum of 0.6 because of a noticeably lower standard error. Due to heterogeneity, we omit the individual Bla28 from the date estimates for Blätterhöhle. For our main analyses, we also omitted the outlier Protoboleráz individual GEN61, yielding an average date of 36.0 \pm 5.3 generations, to help capture uncertainty due to the disagreement between the individual-level and group-level estimates shown here. Average sample dates (except for Körös) are based on the same weighting as the individual-level average dates of admixture for compatibility (Supplementary Information section 7).



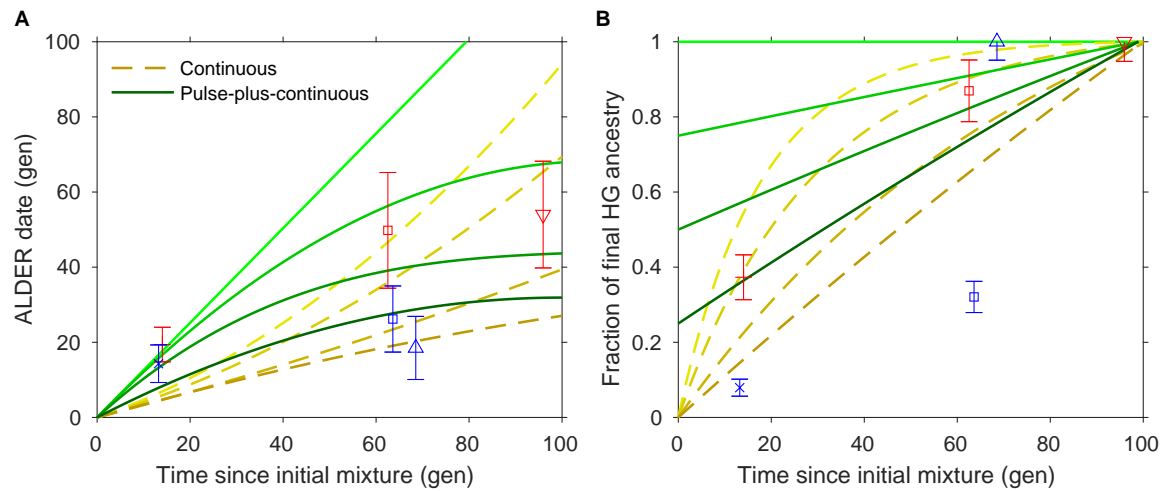
Extended Data Figure 1. First two principal components from PCA. We merged with populations genotyped on the Affymetrix Human Origins array and computed PCs for a set of 826 present-day western Eurasian individuals (background gray points). We then projected ancient individuals using the “lsqproject” and “shrinkmode” options in smartpca [26]. Shown is a closeup omitting the present-day Bedouin individuals.



Extended Data Figure 2. Hunter-gatherer ancestry as a function of latitude and longitude for Neolithic individuals from (A), (B) EN/MN Hungary; (C), (D) LN/CA Hungary; and (E), (F) Iberia. Protob., Protoboleráz.



Extended Data Figure 3. Scaffold admixture graph used for modeling European Neolithic populations. Dotted lines denote admixture events. Anatolia Neolithic, LB1, and KO1 are modeled as admixed, with Basal Eurasian ancestry, deeper European hunter-gatherer ancestry, and FEF ancestry, respectively. European test populations are fit as a mixture of FEF and ancestry related to one or two of the four WHG individuals (here Villabruna-related as an example). See Supplementary Information section 6 for full details.



Extended Data Figure 4. Admixture dates (A) and proportions (B) as a function of time for the Germany (blue) and Iberia (red) time series and simulated data, as in Figure 3. Symbols are as in Figures 1 and 2, here showing population-level averages plus or minus two standard errors. Proportions and standard errors in (B) are normalized by the total hunter-gatherer ancestry in the most recent (rightmost) population in each region. Yellow dashed lines represent continuous admixture simulations: from top to bottom, diminishing 5% per generation, diminishing 3%, diminishing 1%, and uniform. Green solid lines represent pulse-plus-continuous admixture simulations: from top to bottom, all hunter-gatherer ancestry in a pulse at time zero; 3/4 of final hunter-gatherer ancestry in an initial pulse, followed by uniform continuous gene flow; 1/2 in initial pulse and the rest continuous; and 1/4 in initial pulse.